

LIDAR

Exploiting the Versatility of a measurement principle in Photogrammetry

Norbert Pfeifer

Department of Geodesy and Geoinformation

TU Wien

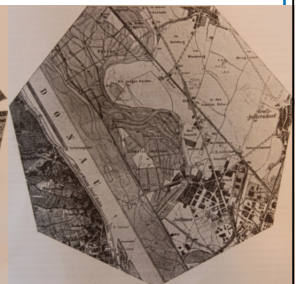
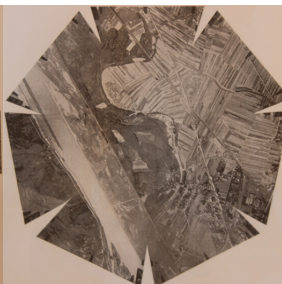
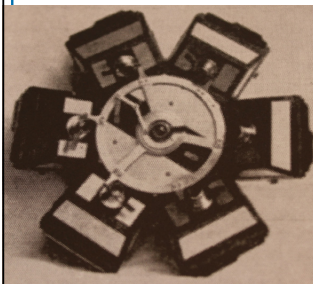


Photogrammetry and cameras

- TU Wien, 200th anniversary
November 6, 1815: k. k. polytechnisches Institut in Wien

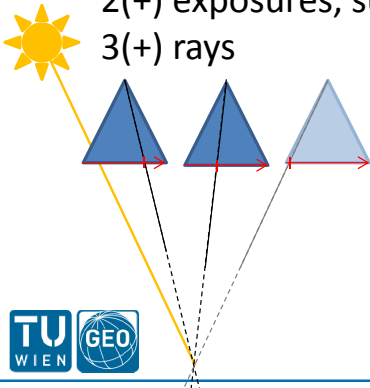


- Theodor Scheimpflug, 1865-1911: 150th anniversary

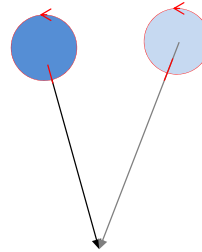


Cameras and Laser Scanners

- Measurement of angles/directions
- Measurements in focal plane simultaneous
- 3D point reconstruction: 2(+) exposures, sun light = 3(+) rays



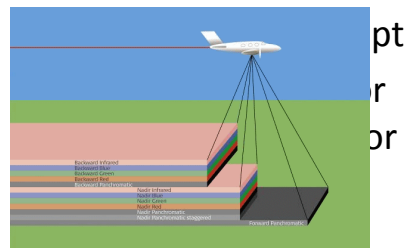
- Measurement of angles/directions and range
- Sequential measurements
- 3D point reconstruction: 1(+) scan = 1(+) vector



Cameras and Laser Scanners

Other differences and convergence

- Size of aperture & resolution limit
- Sampling (under-, contiguous, over-sampling)
- Push broom cameras and flash lidar sensors



- Area-wise sampling of

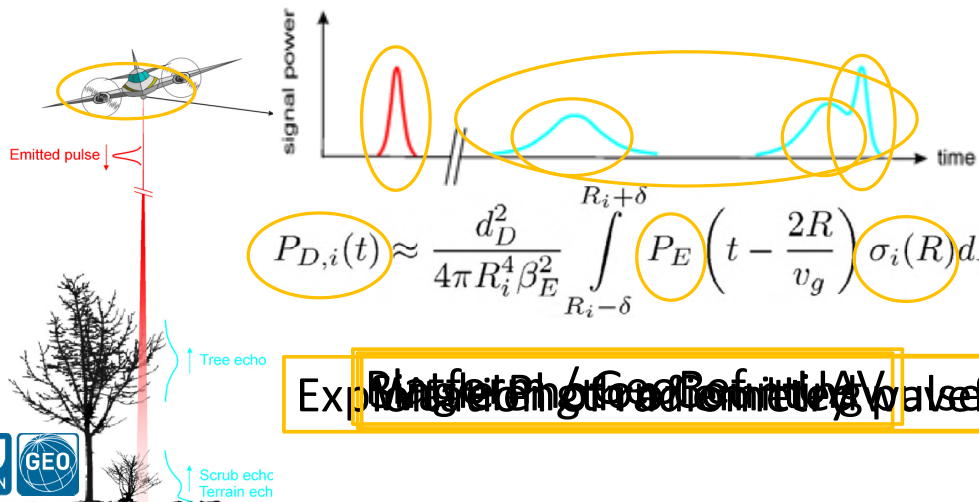


- Resolution with

Laser scanning is the polar photogrammetry ...

... beyond rays vs. vectors

- Laser Range Finder → Light Detection and Ranging
- Lidar principle
 emission of a laser pulse and
 time resolved detection and analysis of its echo
 to infer properties of the reflecting objects (targets, reflectors, ...)

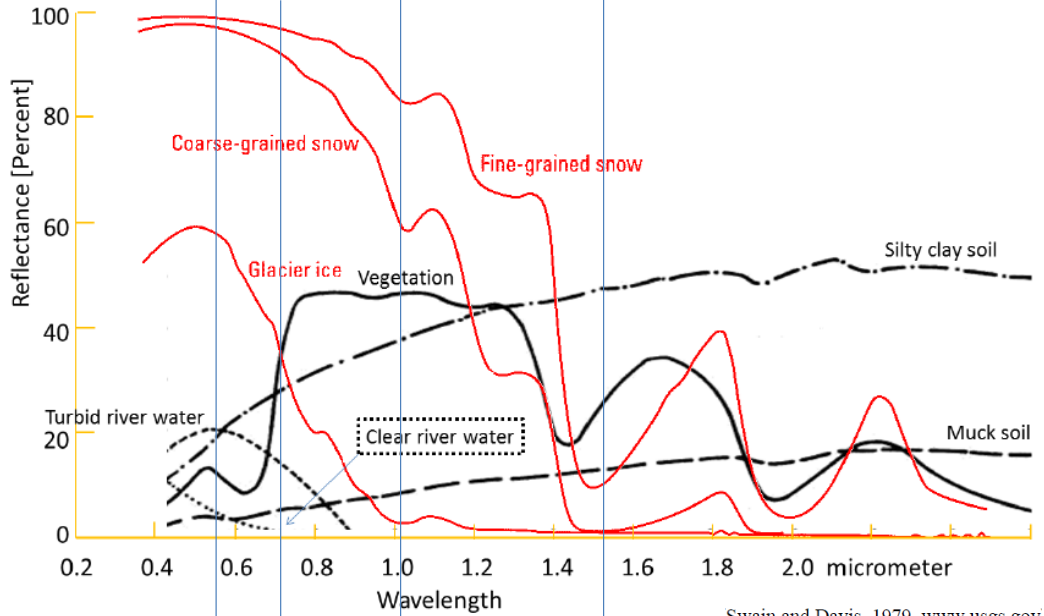


Exploiting the full waveform

The Versatility of Lidar

- Wavelength of the emitted pulse
 Lidar bathymetry
 Case study on river dynamic morphology
- Full waveform recording
 Waveform analysis and radiometric calibration
 Case study on bi-temporal classification of grass-land
- Single photon counting
 Towards Lidar from space
- Platform developments
 Case study on measurement of vegetation parameters
- Additionally exploited in (e.g.) atmospheric remote sensing:
 frequency shift of the backscatter, polarization, ...

Reflectance and LiDAR wavelength



Swain and Davis, 1979, www.usgs.gov



532nm bathymetric
690nm terrestrial
1064nm airborne
1550nm +terrestrial topographic

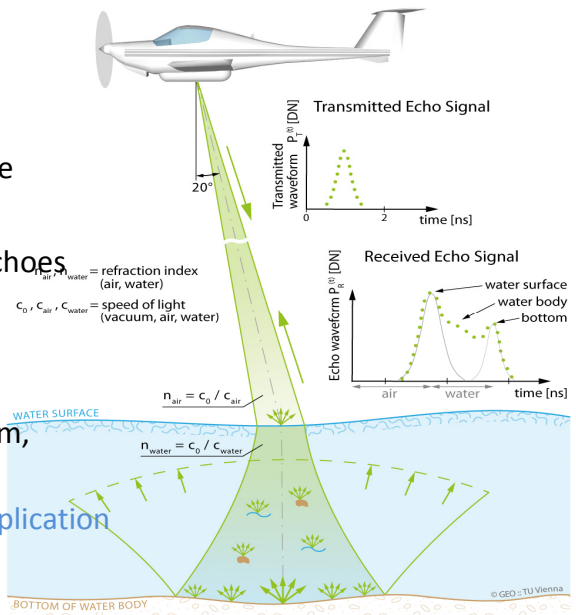
Bathymetric Lidar

Challenges to Understanding

- Backscatter from water surface, relation of water properties, effect on echo time lag and shape

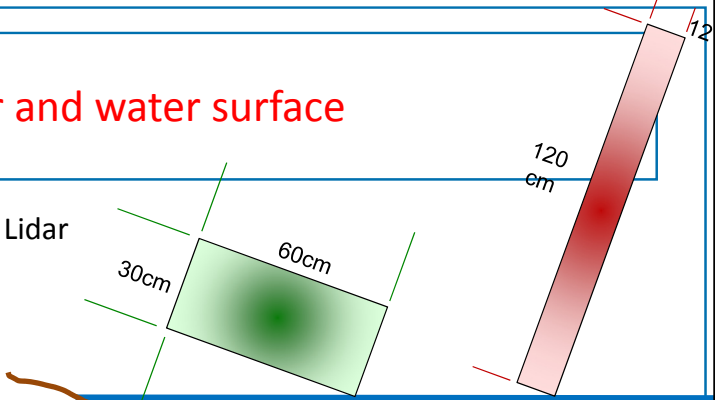
Challenges in Processing

- Identification of water surface echoes
- Modeling of water surface for application of Snell's law
- Classification of echoes: Foreland, vegetation, river bottom, water column reflectors, etc.
- Suitable modeling for specific application

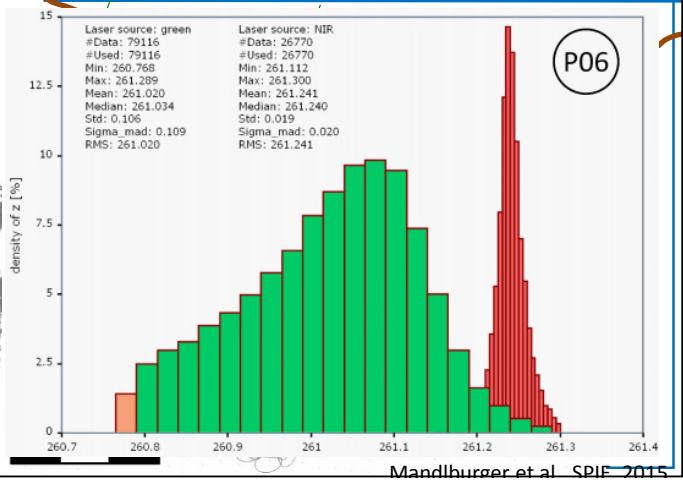
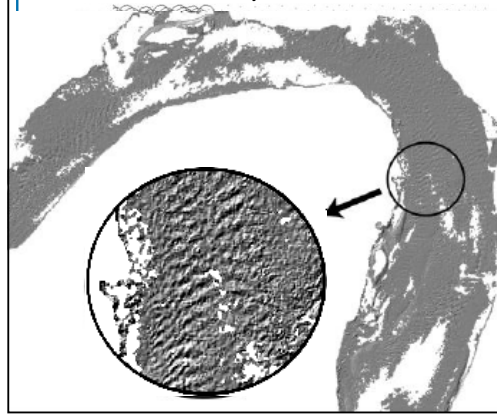


Lidar and water surface

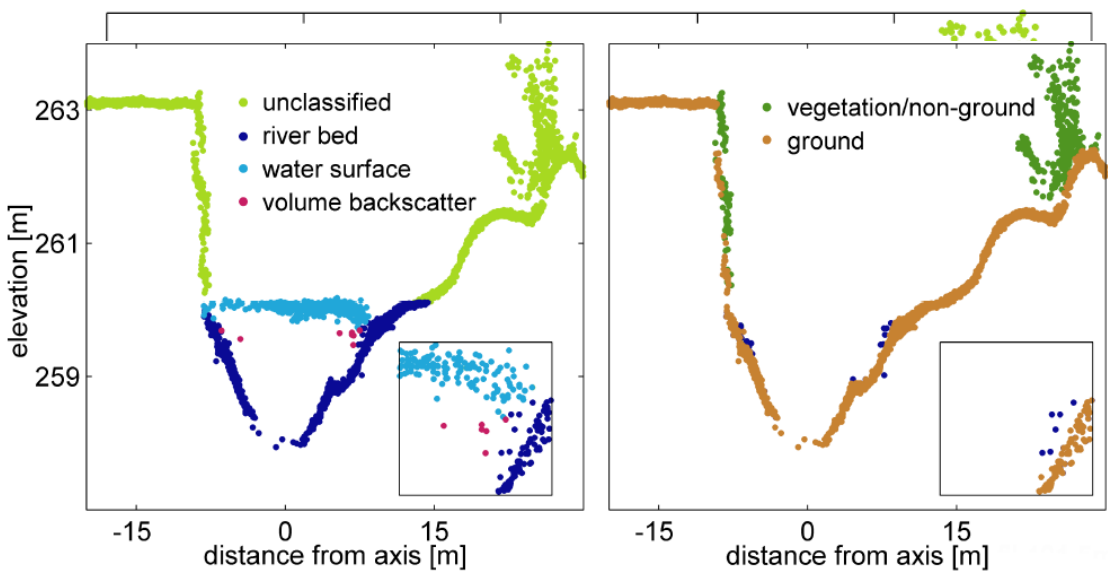
- Difference to topographic Lidar shape of emitted pulse typical example

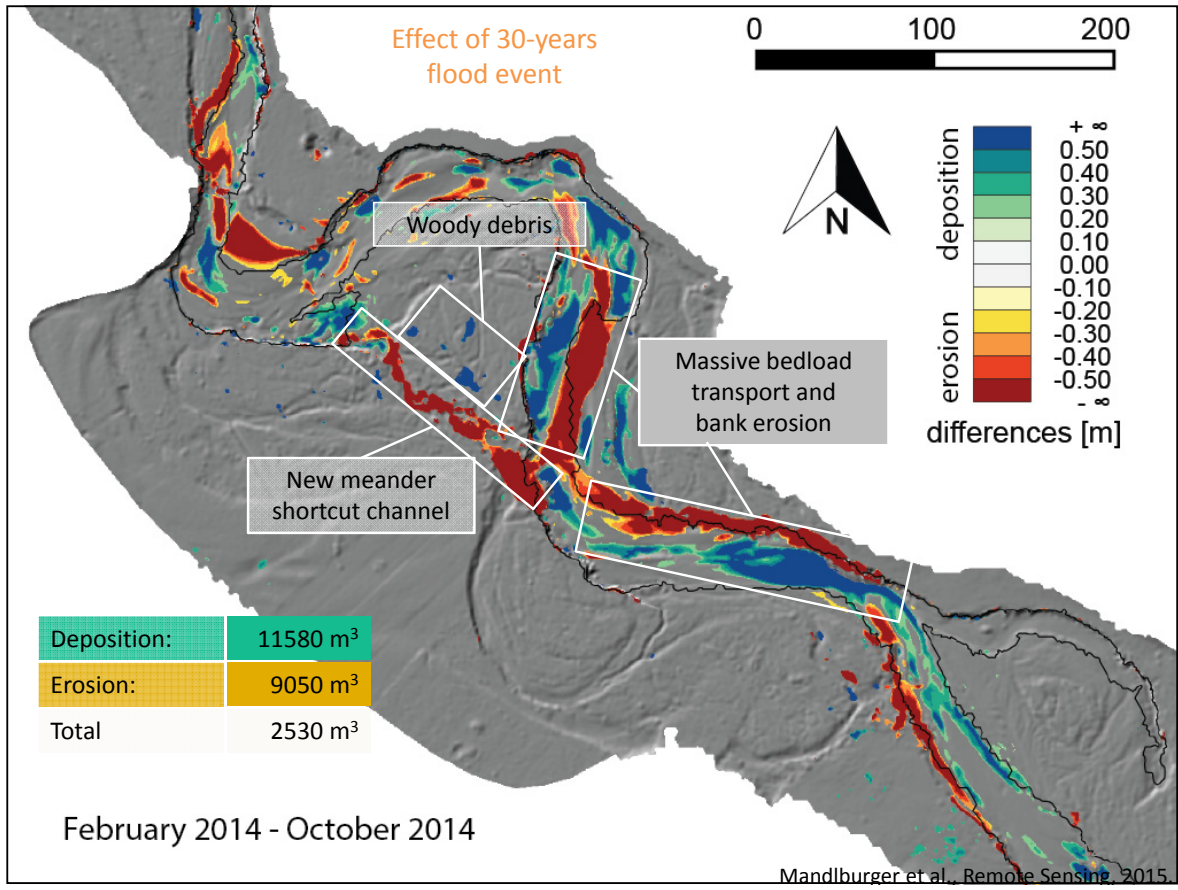
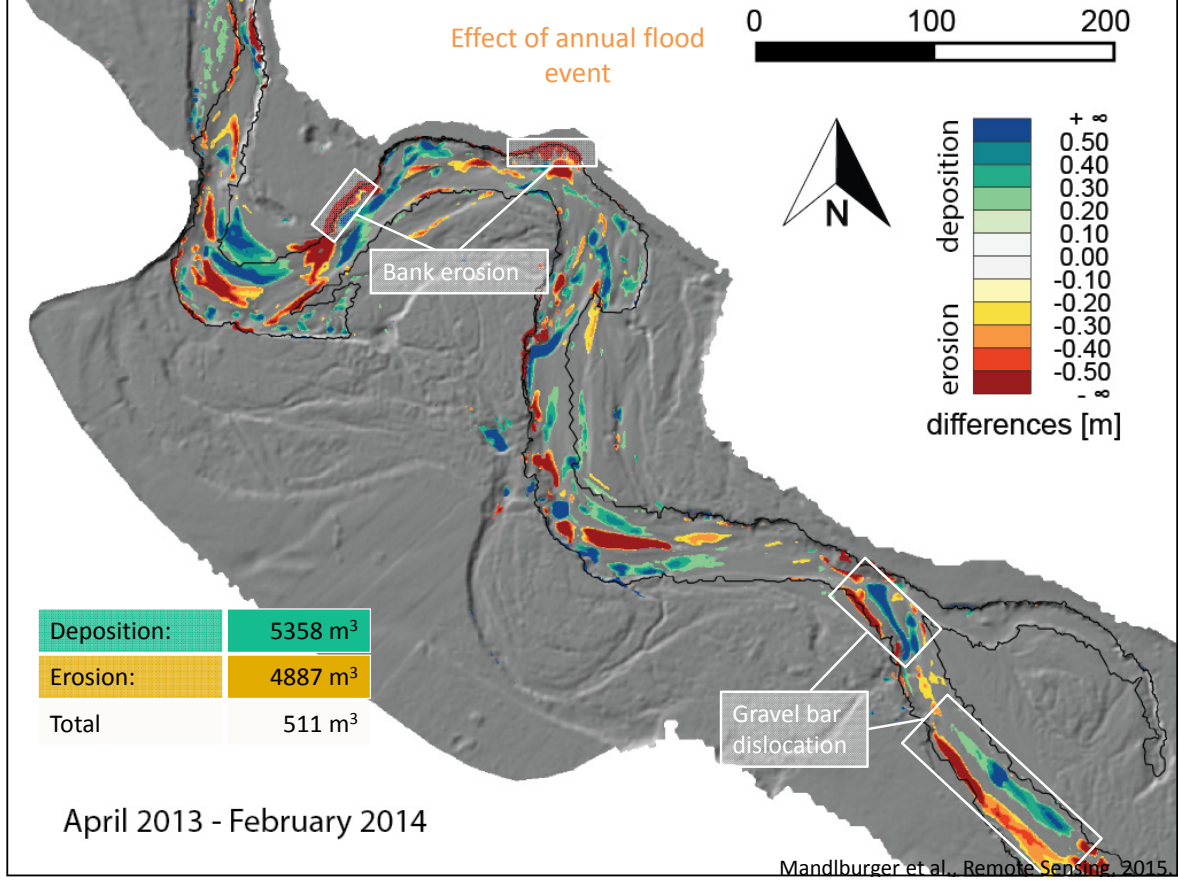


- Case study on river bank

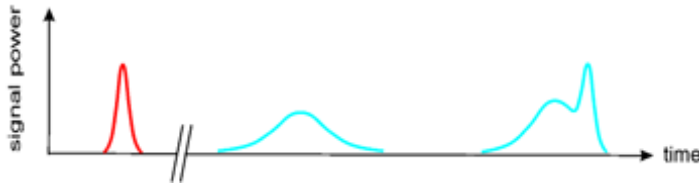


Processing and modeling of bathymetric point clouds





Waveform analysis and exploitation



$$P_{D,i}(t) \approx \frac{d_D^2}{4\pi R_i^4 \beta_E^2} \int_{R_i-\delta}^{R_i+\delta} P_E \left(t - \frac{2R}{v_g} \right) \sigma_i(R) dR$$

- Amplitude of emitted pulse and backscattered echoes are sampled
 $\Delta t = 0.5 \text{ ns} - 2 \text{ ns}$
- Waveform recording allows radiometric calibration
Measurement at sensor \rightarrow reflection properties of objects
- Established (e.g.) to strongly support differentiation between low vegetation and ground/solid objects (terrain in forest, deadwood, ...)



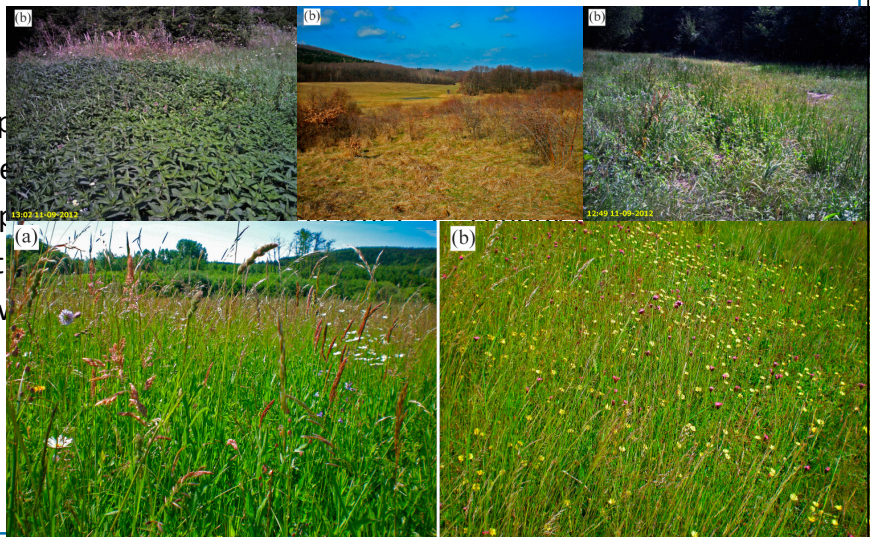
Waveform: exploitation of radiometric and geometric measurements

Study on the classification of grass land

- 10 classes, including fringe, abandoned, meadow-like, lowland hay meadow, dry meadow

Exploitation of

- waveform shape
- radiometric measurements
- geometric properties
- geometric texture
- difference between



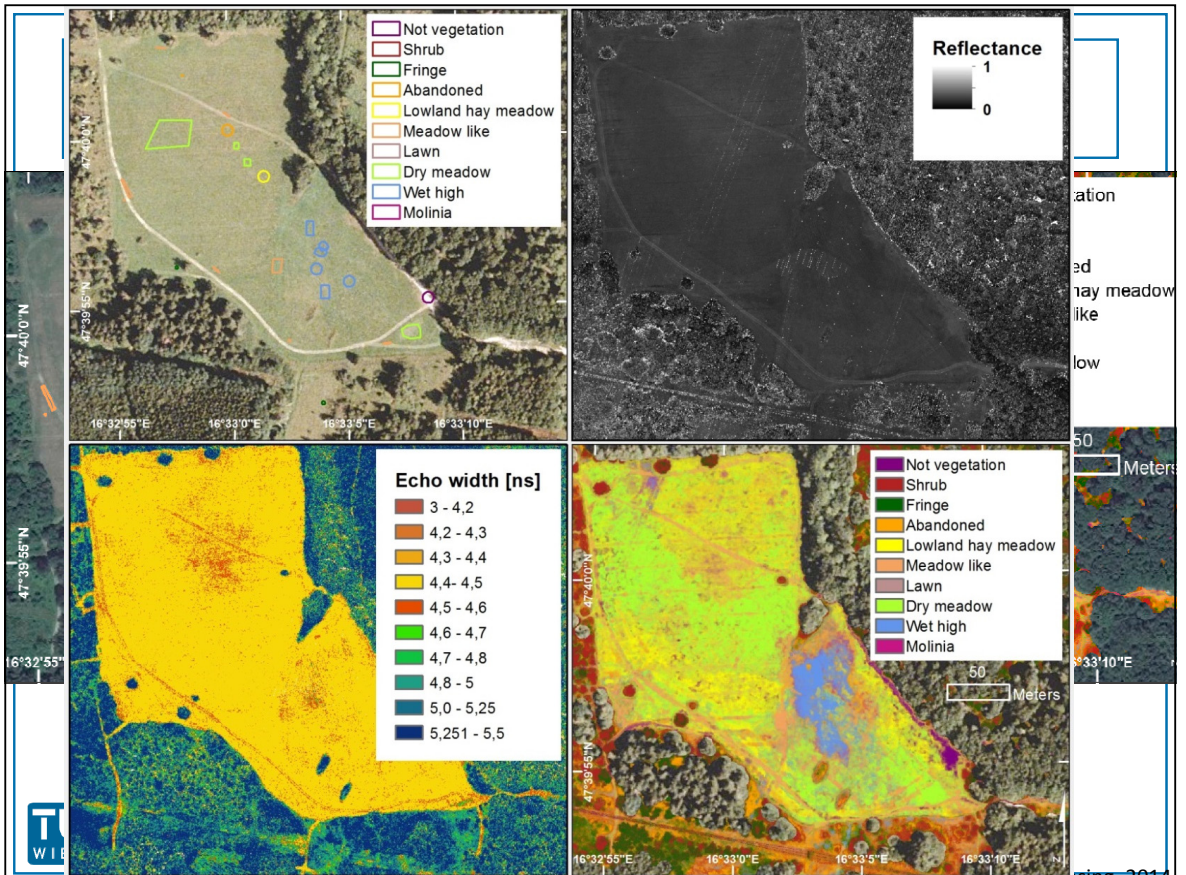
Waveform: exploitation of radiometric and geometric measurements

Classification

- Decision trees
- Machine learning based on ground reference data
- Determine class and probability (on pixel basis)

Most important bands according to classifier

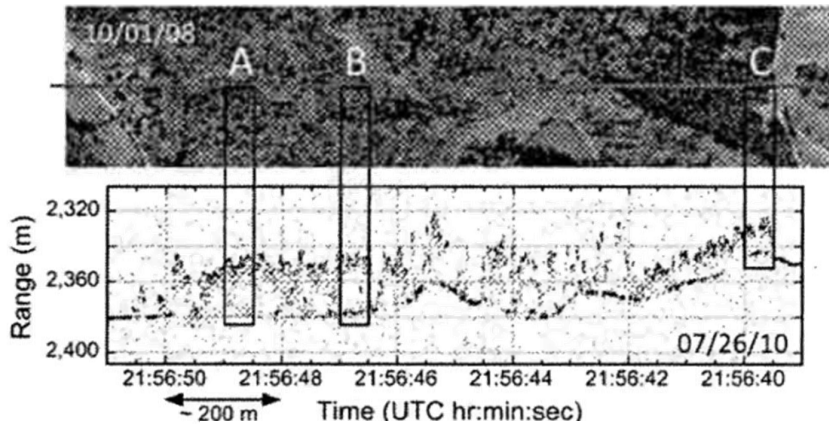
- Leaf off echo width, difference between leaf on/leaf off reflectance, leaf off nDSM height



Detection: Single Photon Counting

Large „flying“ heights, lidar on space-borne platforms

- Strong signals required for weak return signals
- Therefore, single photon detection



Airborne demonstration of SPC measurements

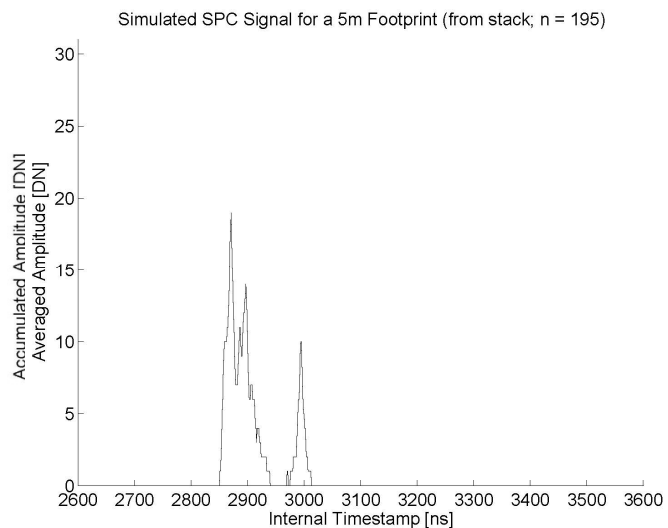


Harding et al., 2011. Polarimetric, two-color, photon-counting laser altimeter measurements of forest canopy structure. International Symposium on Lidar and Radar Mapping 2011: Technologies and Applications, 8286

Single Photon Counting / Simulation



Simulated return of 5m footprint, SPC

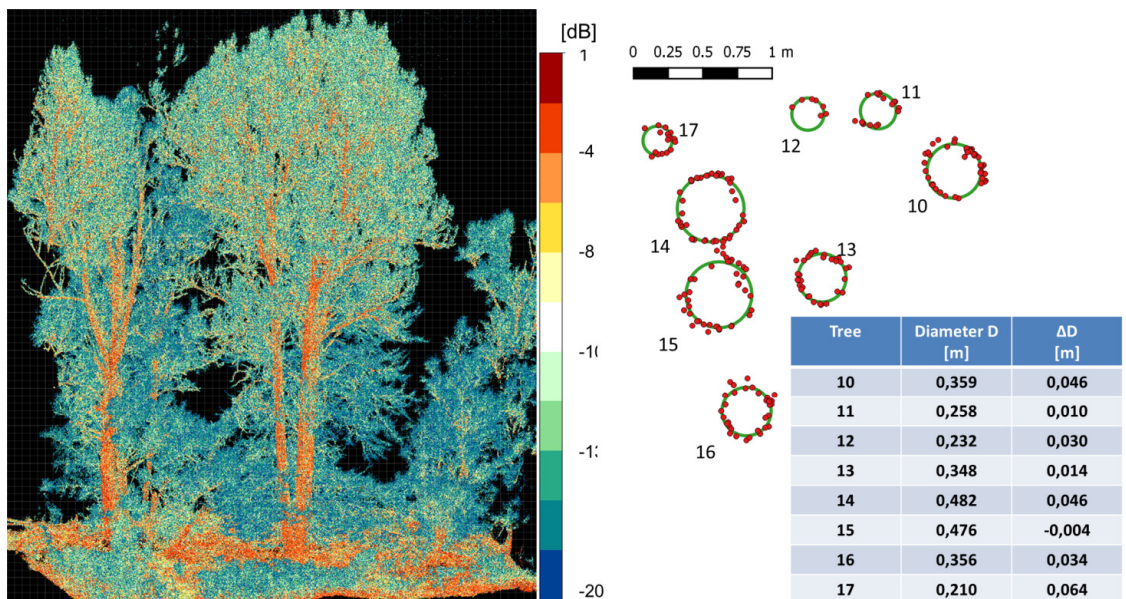


UAV as platform for Lidar



Image: Riegl

Modeling of tree diameter from UAV Lidar



Relative reflectance
Mandlbürger et al., GIM, 2015

Data provided by Riegl

Take home message

- Lidar provides more than (multiple) ranges along the direction of imaging rays
- Additional observations (echo width, reflectance, ...) for land cover classification / object detection
- Wavelength choice adapted to studied phenomenon or process
e.g. water
will become importance for classification (multi wavelength case)
- SPC (and also beam deflection) studied by space agencies for global lidar coverage
- Correct interpretation of point clouds requires knowledge about footprint size
- Very high resolution dynamic lidar point cloud acquisition will require refined models of strip adjustment



Literature

- Mandlbürger et al., SPIE, 2015:
Mandlbürger, Pfennigbauer, Riegl, Haring, Wieser, Glira, Winiwarter, 2015: Complementing airborne laser bathymetry with UAV-based lidar for capturing alluvial landscapes. SPIE (forthcoming)
- Mandlbürger et al., Remote Sensing, 2015:
Mandlbürger, Hauer, Wieser, Pfeifer, 2015: Topo-Bathymetric LiDAR for Monitoring River Morphodynamics and Instream Habitats—A Case Study at the Pielach River. Remote Sensing, 2015, 7.
- Zlinszky et al., Remote Sensing, 2014:
Categorizing Grassland Vegetation with Full-Waveform Airborne Laser Scanning: A Feasibility Study for Detecting Natura 2000 Habitat Types. Remote Sensing, 2014, 6.
- Mandlbürger, Glira, Pfeifer, 2015:
UAS-borne Lidar for Mapping Complex Terrain and Vegetation Structure. GIM International, 29.

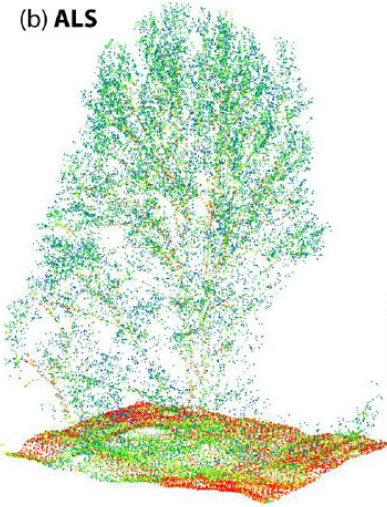


Comparison of point clouds

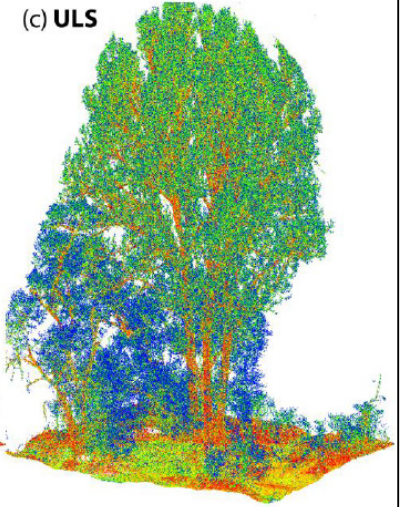
(a) ALB



(b) ALS

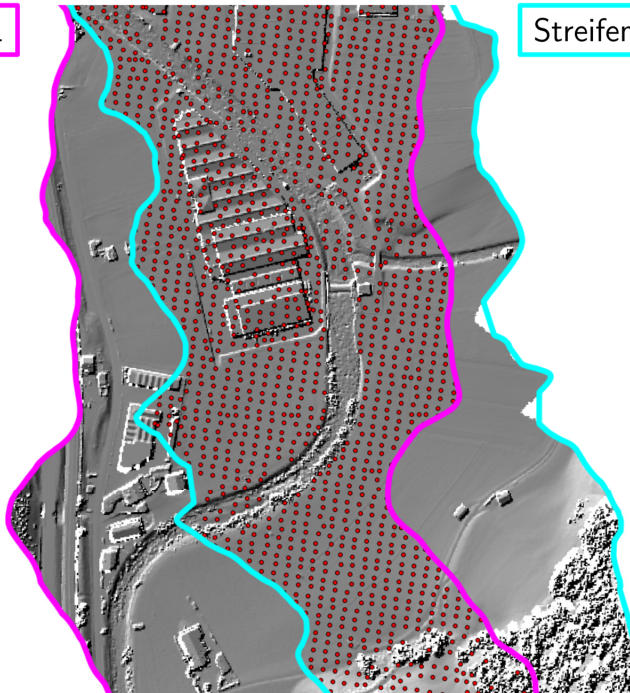


(c) ULS



Mandlbauer et al., SPIE, 2015.

Streifen 1

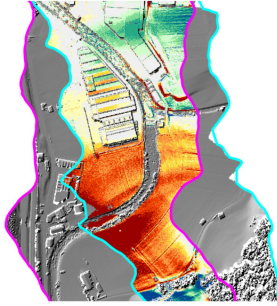


Streifen 2

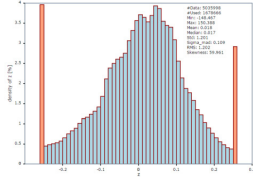


Rot = Korrespondenzen

1 keine zeitabhängige Korrektur der Trajektorie

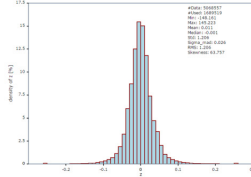
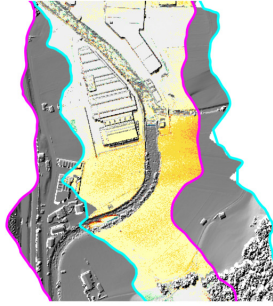


Histogramm mask. Streifendiff.:



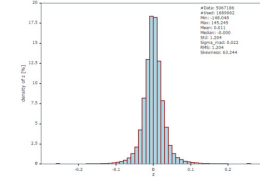
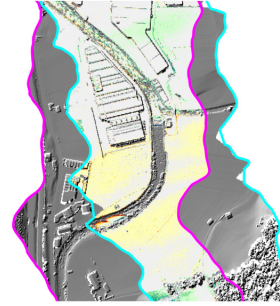
median = 1.7 cm
sigma_mad = 10.9 cm

2 zeitabhängige Korrektur mit $\Delta t = 60$ s

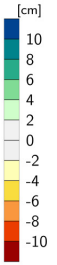


median = -0.1 cm
sigma_mad = 2.6 cm

3 zeitabhängige Korrektur mit $\Delta t = 30$ s

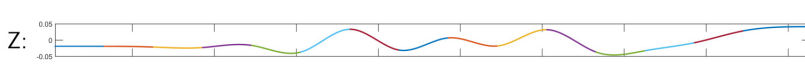
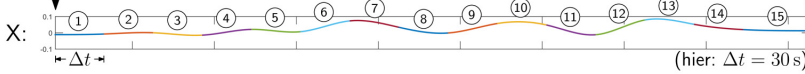


median = 0.0 cm
sigma_mad = 2.2 cm

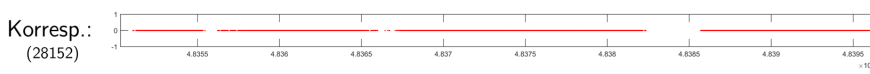
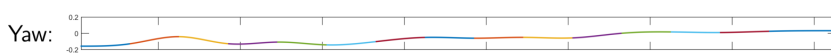
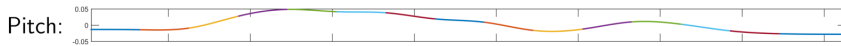
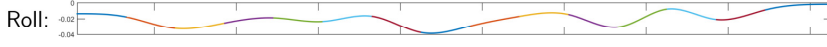


Korrektur
Position

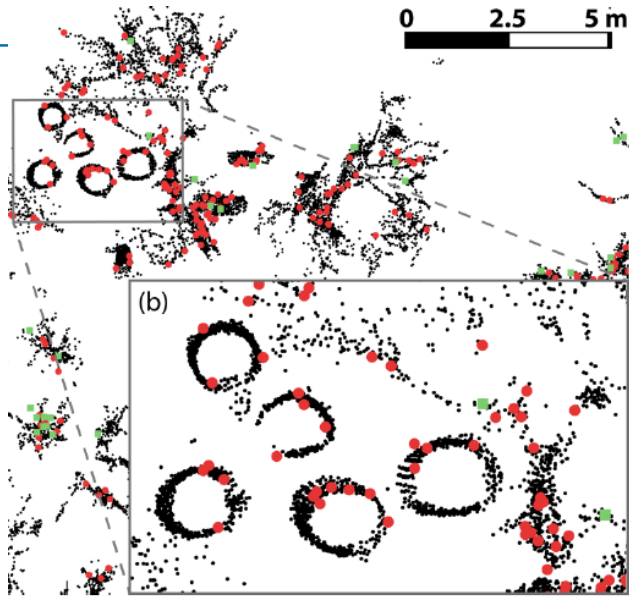
Startzeit Endzeit



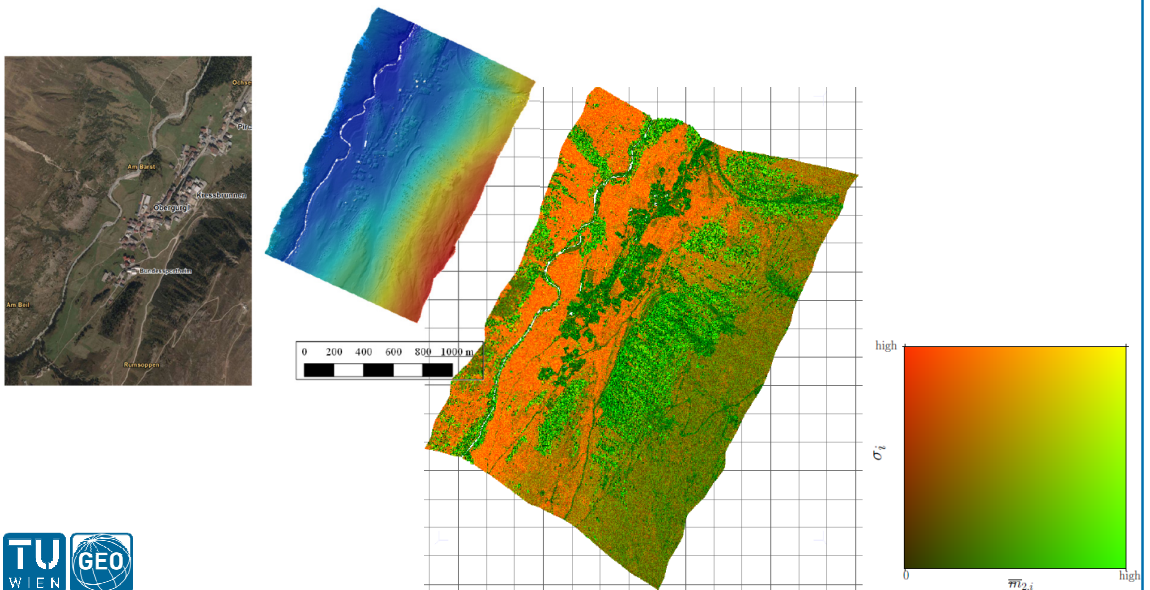
Korrektur
Winkel



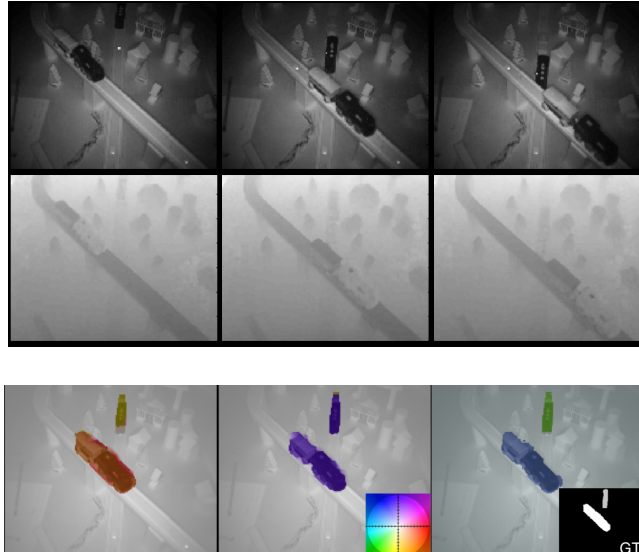
Bedingungen: C1-,C2-,C3-Stetigkeit, 1. und 2. Abl. = 0 zu Start- und Endzeit



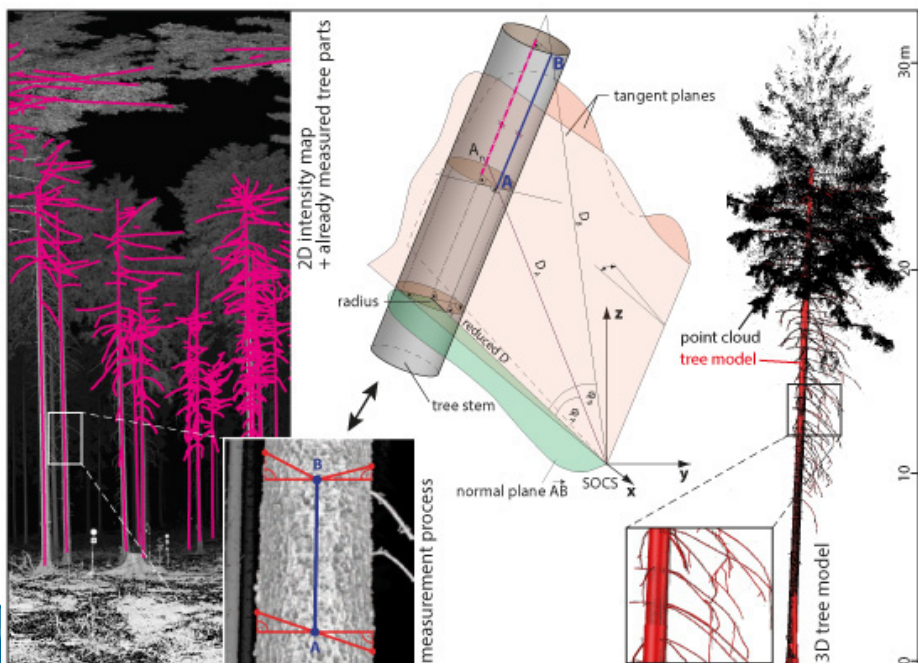
FWF-Signale rückfalten zur Objektcharakterisierung



Pixel, Bewegungsrichtung, Trajektorie, Segmente in Raum und Zeit



Baummodelle aus TLS Punktwolken im Wald (für RT)

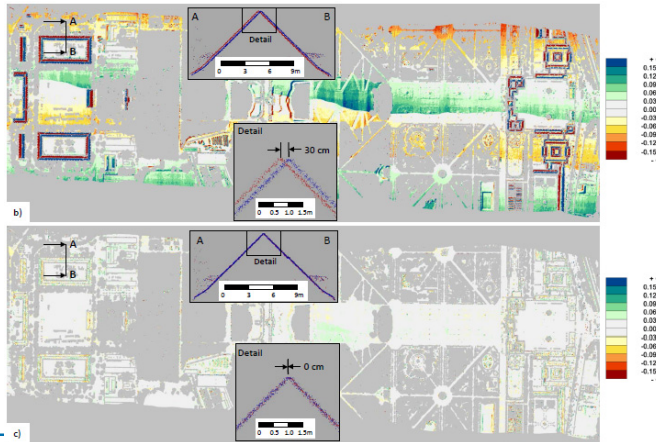


Punktwolken: Review (paper) und Prozessierung (software)

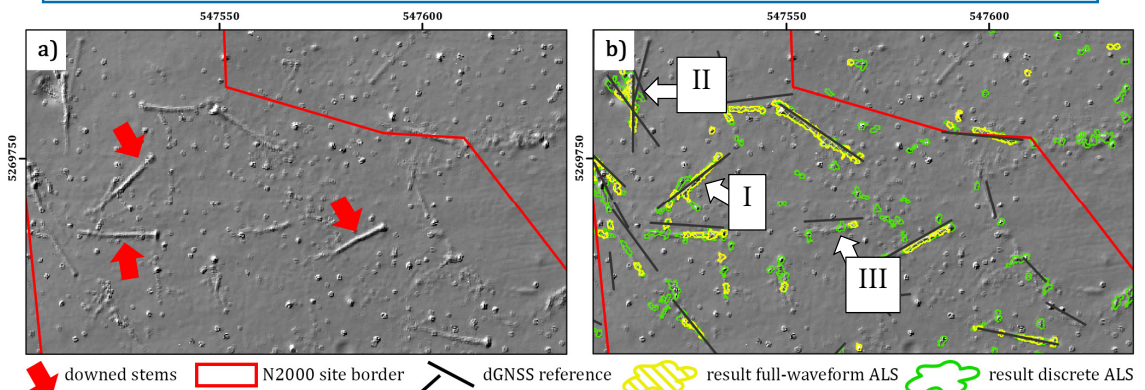


(a) LiDAR data

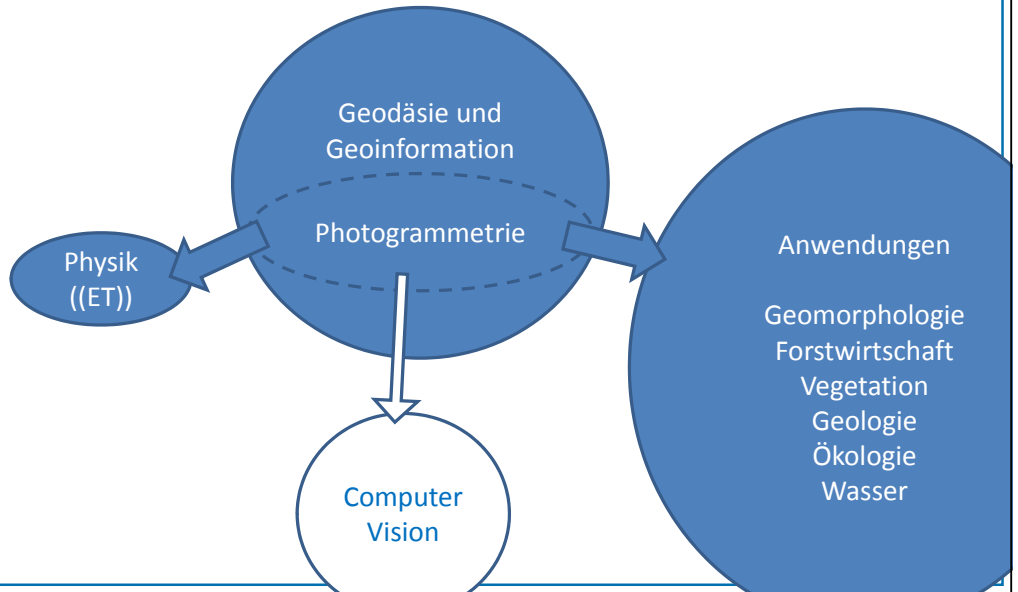
(b) Dense matching



Liegendes Totholz aus FWF Airborne Laserscanning



Forschung – Konzept



Fringe (e.g. *Urtica*), abandoned (e.g. woody encroachment), meadow like (e.g. timber storage and traffic), lowland hay meadow, dry meadow

